Journal of Hydrology: Regional Studies 40 (2022) 101002

Contents lists available at ScienceDirect

Journal of Hydrology: Regional Studies

journal homepage: www.elsevier.com/locate/ejrh

The lake-level changes of Lop Nur over the past 2000 years and its linkage to the decline of the ancient Loulan Kingdom

Yun Shao [a,b,h], Huaze Gong [a,b], Charles Elachi [c], Brian Brisco [d], Jiaqi Liu [e], Xuncheng Xia [f], Huadong Guo [a], Yuyang Geng [a,b,h], Shugang Kang [g], Chang-an Liu [a,h], Zhi Yang [a,h], Tingting Zhang [a,b,*]

[a] *Aerospace Information Research Institute, Chinese Academy of Sciences, Beijing 100094, China*
[b] *Laboratory of Target Microwave Properties, Deqing Academy of Satellite Applications, Zhejiang 313202, China*
[c] *California Institute of Technology, 1200 East California Boulevard, Pasadena, CA 91125, USA*
[d] *Canada Centre for Remote Sensing, Natural Resources Canada, 560 Rochester Street, Ottawa, Ontario K1A 0E4, Canada*
[e] *Institute of Geology and Geophysics, Chinese Academy of Sciences, Beijing 100029, China*
[f] *Xinjiang Institute of Ecology and Geography, Chinese Academy of Sciences, Xinjiang 830011, China*
[g] *State Key Laboratory of Loess and Quaternary Geology, Institute of Earth Environment, Chinese Academy of Sciences, Xi'an 710061, China*
[h] *University of Chinese Academy of Sciences, Beijing 100049, China*

ARTICLE INFO

Keywords:
Lop Nur
Loulan Kingdom
SAR remote sensing
OSL dating

ABSTRACT

Study region: Lop Nur, Xinjiang Province, China
Study focus: Lop Nur has been a vast playa which was a historic lake in eastern Tarim Basin, northwest China. The lake's catchment played a significant role in the development of oasis states in the early Common Era, such as the ancient Loulan Kingdom. However, the history of lake dynamics remains unclear, and its potential linkage to the decline of Loulan Kingdom has been not well-examined. This paper aims to reconstruct the lake-level changes in Lop Nur over the last 2000 years using synthetic aperture radar (SAR) data, optically stimulated luminescence (OSL) dating of lacustrine and aeolian sediments, and radiocarbon (^{14}C) dating of ancient bio-remains. Furthermore, the relationships between Lop Nur' fluctuation and the decline of ancient Loulan Kingdom were discussed
New hydrological insights for the region: The results suggest that Lop Nur once covered an area more than 11, 602 km^2 and that lake-level reduced gradually during 360–470 C.E. Subsequently, the lake experienced a few stages of lake-level fluctuation which never reached the upper-most shorelines. Also, the historical changes in the lake level were temporal coincided with the ancient Loulan Kingdom's collapse, showing that the dynamics of hydrological conditions in catchment may have a direct influence on the fall of human settlement in drylands.

1. Introduction

Lop Nur, located at the east end of the Tarim Basin, received most of the drainage from the Tianshan and Kunlun Mountains until the 1970s, when Lop Nur eventually desiccated (Mischke et al., 2017; Zhang et al., 2014, 2021). During the Han Dynasty (206 B.C. E.–220C.E.), Lop Nur was a large lake located on the eastern side of the Loulan Kingdom (89°55′22″E , 40°29′55″N) (Li et al., 2019;

* Corresponding author at: Aerospace Information Research Institute, Chinese Academy of Sciences, Beijing 100094, China
E-mail address: zhangtt201832@aircas.ac.cn (T. Zhang).

https://doi.org/10.1016/j.ejrh.2022.101002
Received 27 July 2021; Received in revised form 13 January 2022; Accepted 15 January 2022
Available online 18 January 2022

Yang et al., 2006a; Yu, 2014). The Loulan Kingdom existed as early as 176 B.C.E. (Chen, 2014; Xia et al., 2007). Historical records and ruins discovered in the territory show that the region was once the political, military, economic, and cultural center of western China. It was positioned along the Central Route of the ancient Silk Road that connected China to Europe and Central Asia between 77 B.C.E. and 500 C.E. (Li et al., 2021a). However, the Loulan Kingdom vanished abruptly around 1500 years ago (Qin et al., 2011; Xu et al., 2017).

The factors leading to the demise of the Loulan Kingdom have not been fully identified and its disappearance has resulted in a considerable and ongoing debate. Proposed causes of its demise have included climate change (aridification), a change in the river course of the Tarim River, abandonment of this route of the ancient Silk Road, and various human activities such as war and feuds over water for irrigation and domestic purposes (Chen, 2014; Mischke et al., 2019; Xia et al., 2007, 2021; Xu et al., 2017). However, climate change is likely to be the most important influencing factor (Xie et al., 2021).

The multi-proxy records of Lop Nur show that humid conditions between 400 B.C.E. and 200 C.E. supported the ancient Loulan Kingdom until aridification began and Lop Nur gradually shrank at 200 C.E. (Liu et al., 2016a, 2016b; Yang et al., 2006a, 2016b). Previous studies have demonstrated that the once-prosperous Loulan Kingdom completely disappeared by about 500 C.E. (Xu et al., 2017). It became a barren landform, even a no man's land, due to a lack of water and intensive wind erosion (Liu et al., 2016a, 2016b; Yang et al., 2006a, 2016b). Evidence demonstrates that irrigated agriculture was widely practiced in the ancient Loulan Kingdom on the west bank of Lop Nur (Qin et al., 2011). Water supply is critical to the survival of all ecosystems on the earth. An extreme climate event, especially an aridification event, may lead to the collapse of a civilization or a kingdom because of its effects on agricultural and pastoral productivity (Blom et al., 1984; Buckley et al., 2010; Büntgen et al., 2011; Chu et al., 2002; Cook et al., 2004; Demenocal, 2001; Elachi et al., 1984; Farr et al., 1986; Hodell et al., 1995; Li et al., 2021b; McCauley et al., 1983; Skonieczny et al., 2015; Turner, 1974; Yancheva et al., 2007). The abandonment of cities in the Tarim Basin and the drying of Lop Nur are attributed to a possible climatic change toward drier conditions around 500 C.E. (Li et al., 2021; Liu et al., 2016a, 2016b; Yang et al., 2006a, 2016b; Zhang et al., 2012, 2013).

Penetration capability is an important advantage of synthetic aperture radar (SAR) remote sensing technology in arid regions. As demonstrated in 1981, the Shuttle Imaging Radar A (SIR-A) mission acquired L-band (25 cm wavelength) HH polarization SAR images worldwide, including images from the Eastern Sahara Desert (Shao et al., 2012). Using the SIR-A images, McCauley et al. (1983) discovered the buried channels of abandoned rivers and other geoarchaeological features in the Eastern Sahara. Their results showed that wave penetration on the order of tens of centimeters in desert soils was common for L-band radar (Shao et al., 2012). Lasne et al. (2009) and Shao et al. (2003) focused on the influence of soil salinity as a function of soil moisture on the dielectric constant of soils and then on the backscattering coefficients. Their study showed that a material with a high-saline moisture content will have both a high real (ε') and an imaginary (ε") dielectric constant and that the material will act as a strong reflector to microwaves. Thus, SAR is highly likely to detect buried, permeable sediments that contain groundwater, such as abandoned river channels and/or lake beds. The echo energy from the strong reflector under the upper low-loss dielectric layer will be strengthened because of the refraction effect of the upper layer (Liu et al., 2016a, 2016b). Polarimetric SAR data contains a tremendous amount of information about its targets (Shao et al., 2012). Previous studies have attempted to develop classic polarimetric algorithms and generate polarimetric parameters that could better describe the targets' characteristics and aid in our understanding of the interaction between microwaves and targets (Touzi, 2004).

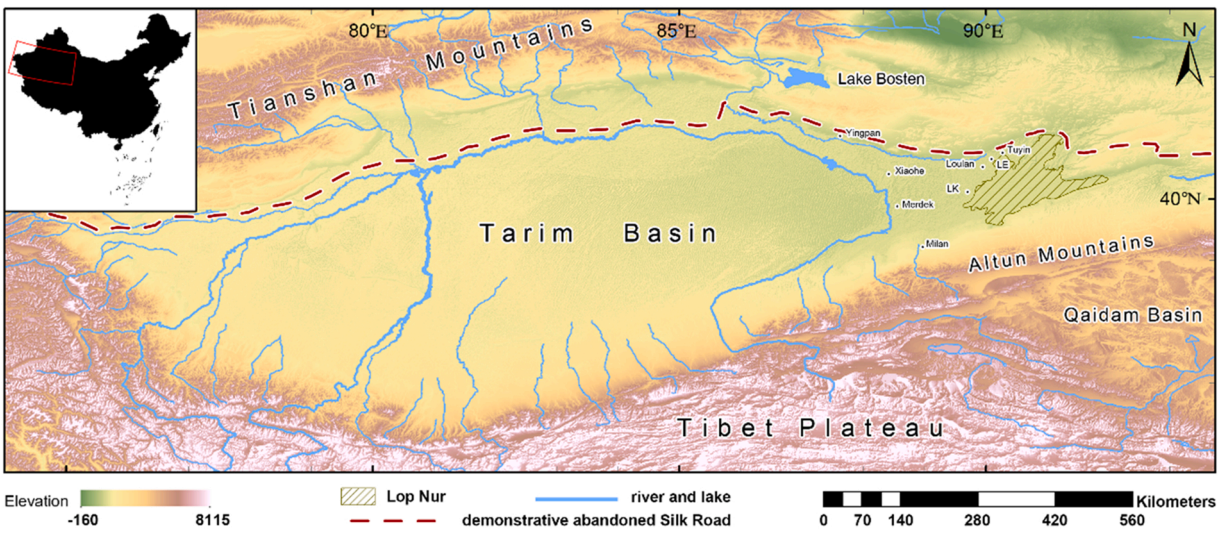

Fig. 1. Location Map of Lop Nur, ruins of cities that existed before the 6th century and adjacent regions, adapted from Zhang et al. (2021). The ruins of Loulan City are 20 km west of Lop Nur; LK City is 60 km south of Loulan City. The abandoned Central Route of the ancient Silk Road is demonstrated by the dashed red line (Frankopan, 2015). (©http://srtm.csi.cgiar.orgwww.dsac.cn).
(For interpretation of the references to colour in this figure, the reader is referred to the web version of this article.).

With the interpretation of spaceborne SAR data, a detailed sequence of shorelines records the historical changes in water levels in Lop Nur was revealed. The paleo-hydrologic reconstruction was carried out based on dating lacustrine and aeolian deposits. The potential link between changes in regional climatic conditions, as indicated by the disappearance of Lop Nur, with the demise of the Loulan Kingdom and the Central Route of ancient Silk Road was examined.

2. Materials and methods

2.1. Study sites

Lop Nur is a vast playa located at the eastern end of the Tarim Basin, northwest China (Fig. 1). The Loulan ruins are about 20 km west of the lake. Nowadays, this region is the aridest part of Eurasia and is very difficult to access (Li et al. (2019a, 2019b)) . The central portion of Lop Nur is best known for being shaped like a human ear, as first seen in the Landsat MSS image acquired in 1972 (Shao et al., 2012). Lop Nur is the lowest region in the Tarim Basin and serves as the basin's depo-center. Before the lake's desiccation, many rivers flowed into Lop Nur, including the Tarim, Kongqi, Tieban, and Qarqan Rivers (Xia et al., 2007). Currently, vast, endless salt crusts are spread over the lake basin and are locally covered by aeolian sediments of various thicknesses. Ten field trips were carried out during 2006–2018. The four dated locations show that Lop Nur has never recovered to its historical highest water level, marked by the upper-most shoreline. The formation of these salt crusts has disrupted the stratigraphic characteristics of the lacustrine and aeolian deposits in most areas, making it challenging to date the deposits (Zhang et al., 2012).

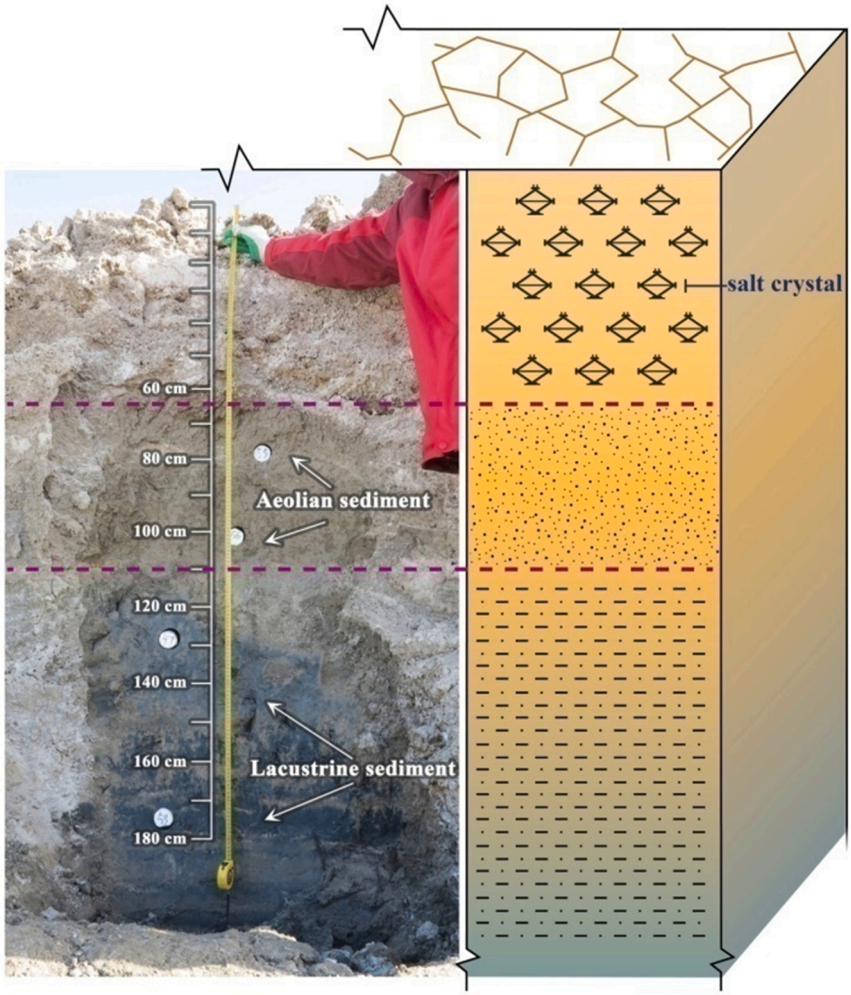

Fig. 2. The stratigraphic section shows typically observed variations in sedimentary deposits and the positions where samples were collected for OSL dating.

2.2. Methods of water level analysis

The analysis of water level changes in Lop Nur was undertaken by (1) using SAR images to define the spatial distribution and elevations of paleo-lake shorelines over the entire extent of the Lop Nur basin, and (2) dating lacustrine and aeolian deposits associated with the shorelines to constrain the age of the shoreline deposits. Each task is described in more detail below.

2.2.1. SAR image interpretation

Several SAR images were used in this study, including C band, RADARSAT of the Canadian Space Agency (CSA), L band ALOS PALSAR of the Japan Aerospace Exploration Agency (JAXA), X band TanDEM-X of the Deutsches Zentrum für Luft-und Raumfahrt, and also GF-1 image of the China National Space Administration. In the Lop Nur basin, the upper layer of salt crust is extremely dry, exhibiting a water content near zero, resulting in a very low complex dielectric constant. However, we found a moist layer beneath the dry upper layer at all sampling sites at depth. As a result, moist saline sediments within Lop Nur appeared as bright features on SAR images. The surrounding geomorphological features, including alluvial deposits, yardang (older lacustrine deposits), bedrocks, and desert areas, have relatively low intensity because of their low dielectric constant (water content near zero) roughness. Thus, the shorelines stand out on the SAR image as bright features because their reflectance differs from the surrounding sediments. When combined with field data, the images identified ancient shorelines that recorded the historical changes in water levels within the lake, even though aeolian sediments buried them. The shorelines appeared as both bright curved features and light grey curved features in the images. Field observations combined with physical/chemical analysis of sedimentary samples revealed that the bright shorelines have higher salt contents than the grey shorelines, while the grey shorelines contain higher sand or silt content (Shao et al., 2012). Due to the autochthonous sedimentary characteristics of Lop Nur, salinity changed little with increasing depth. However, moisture increased abruptly rather than gradually with depth at each sampling site (Li et al., 2015; Wang et al., 2014; Zhang et al., 2014).

The boundary of Lop Nur was defined by interpreting shoreline features on SAR images. The image identifies shorelines defining the lake boundary that are clear in the field. Outside of the lake boundary, the surficial deposits consist of sand and silt, while within the boundary the deposits are dominated by salt crusts. In addition, a Digital Elevation Model (DEM) developed by applying interferometric synthetic aperture radar (InSAR) to TerraSAR-X / TanDEM-X data provides reliable elevation data (Wang et al., 2014) for

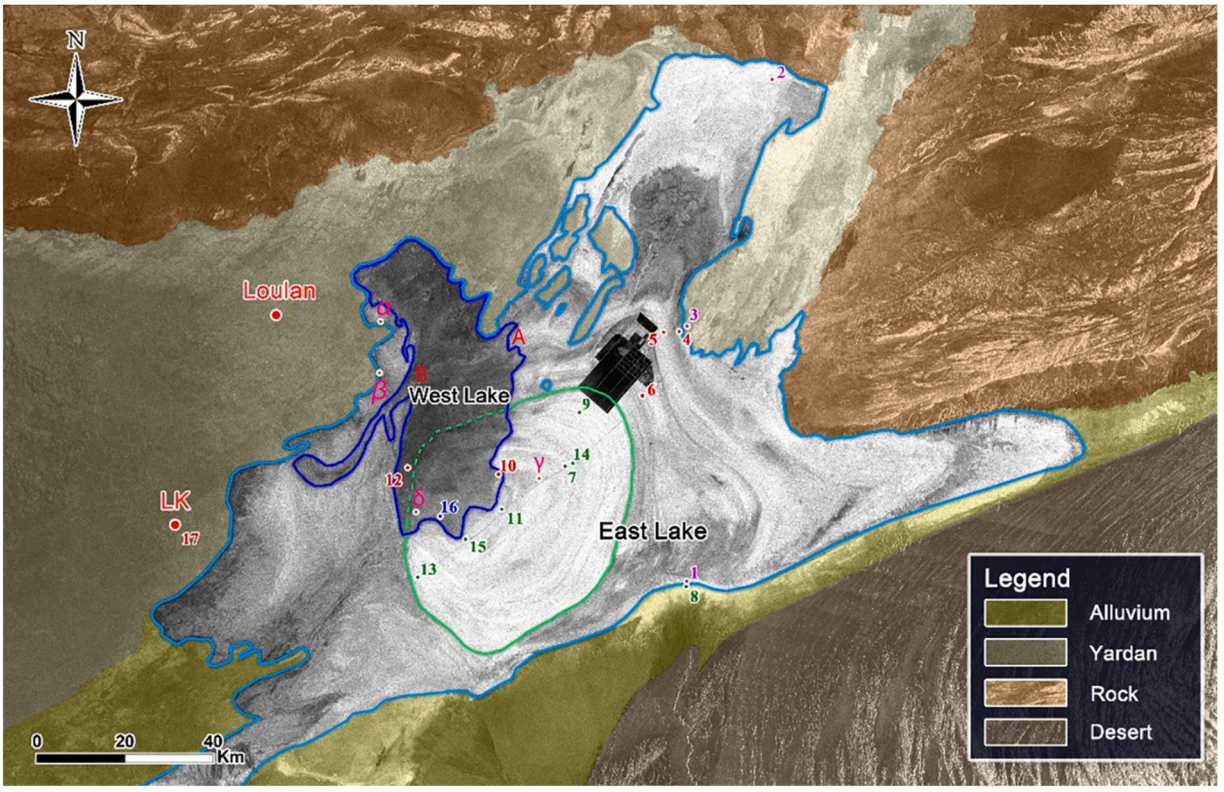

Fig. 3. Interpretative map of Lop Nur based on SAR images ©CSA, ©JAXA. Numbers are sampling sites for OSL and ^{14}C dating. The age of the lake before its desiccation is shown by magenta points, the Lop Nur stage in red, the "ear stage" in green, and the West Lake stage in blue. The light blue line denotes the upper-most shoreline and the largest lake area before 360 C.E.; the green line denotes the "East Lake" area during 641–986 C.E.; the blue line denotes the "West Lake". Alluvial deposits, Yardan, Bedrock, and Desert surround Lop Nur are shown in green, grey, brown, and dark grey shades. Points α, β, γ, δ are ground truth pits for measuring the hardness and roughness of salt crusts. (For interpretation of the references to colour in this figure, the reader is referred to the web version of this article.)

the study area.

Once the distribution of salt crusts identified, the lake boundary was verified in the field at 152 sampling sites for microwave penetration confirming, physical and chemical property analysis (Zhang et al., 2014).

2.2.2. Optically stimulated luminescence (OSL) dating

Landforms observed at these sites were similar, consisting of polygonal patterns of salt crust indicative of arid playas. Suspected shorelines were excavated at each site and sedimentary deposits were delineated, characterized, and sampled. Most sites possessed both lacustrine and aeolian sediments, which were distinguished based on primary sedimentary bedding, color, and particle size distribution. Lacustrine sediments exhibit fine greenish particles, while aeolian sediments are characterized by light yellow particles that are coarser-grained (Fig. 2). Samples for OSL dating were taken from areas where bedding was perpetual and well-defined. Individual beds were at least 20–30 cm thick, had uniform granularity, and lacked erosional features, thereby indicating a stable depositional environment.

In 2013 and 2014, lacustrine and aeolian samples from the subsurface were collected at 23 sampling sites across the entire Lop Nur. Only 16 sampling sites had dateable samples. The 16 sampling sites are projected onto the georeferenced SAR images (Fig. 3). We deliberately collected aeolian sediments that overlaid the uppermost lacustrine deposits as indicators of the onset of dry conditions within the lake basin (Fig. 4). The aeolian deposit represented when the lakebed was exposed after desiccation and the windblown sediments reached the sampling sites.

We intended to date all sediment layers within the excavated pits, but the re-growth of salt crusts, a normal phenomenon in playas with shallow groundwater brines, led to the destruction of stratigraphic bedding. Moreover, most samples are composed of high salt content. Over 90% salt content is common in the Lop Nur basin. Thus, it was extremely difficult to collect sediment samples for geochronological analysis. As a result of salt crystallization, many of our collected samples were “contaminated” by the mixing of sediments between layers.

Quartz OSL dating was conducted at the Institute of Earth Environment, Chinese Academy of Sciences. The luminescence sample tubes were processed under dim red-light conditions in the laboratory. The sediments at the two ends of the tube were removed because they may be exposed to daylight during sampling. The remaining loess sample was prepared for equivalent dose (De) determination and radioisotope (U, Th, and K) concentration analysis. On the Chinese Loess Plateau, the fine-grained (4–11 μm) quartz was extracted using the pretreatment procedures for loess (Kang et al., 2018). The samples (~50 g) were first treated with 30% H_2O_2 and 30% HCl to remove organic materials and carbonates, respectively. The samples were washed with distilled water until they

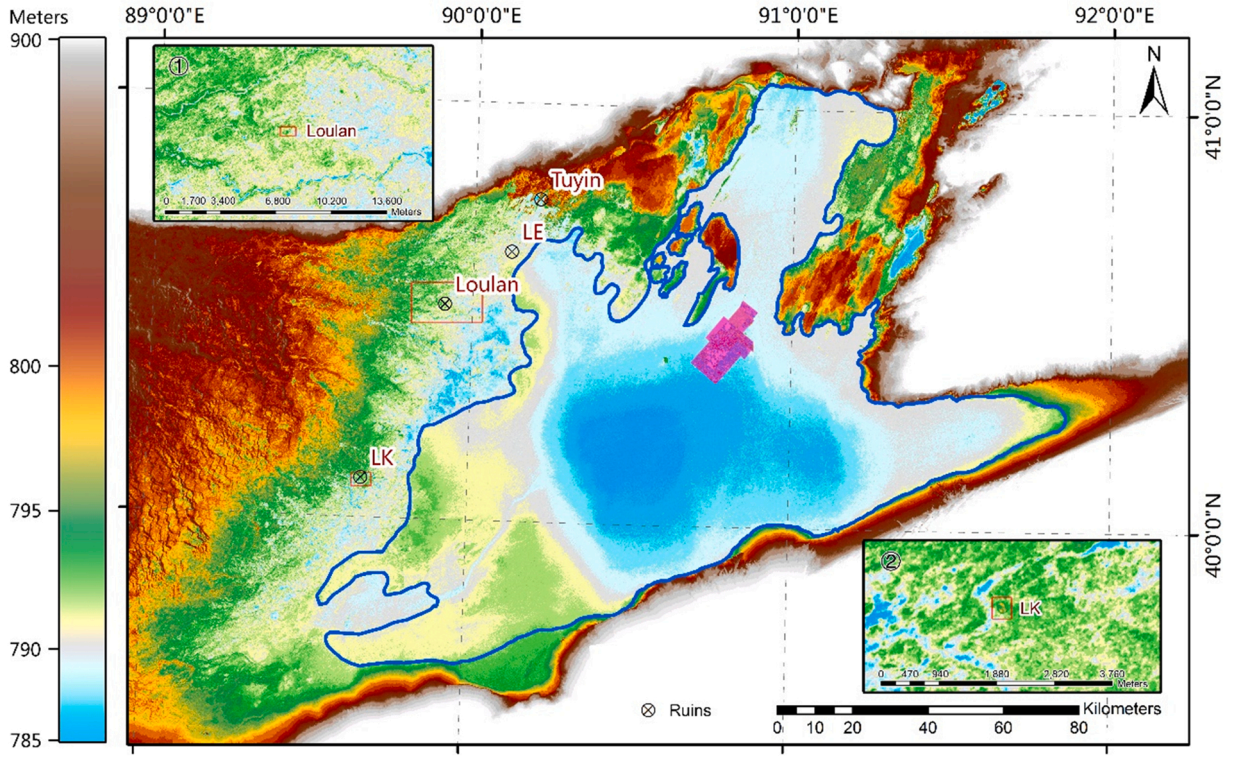

Fig. 4. TanDEM-X DEM of Lop Nur adapted from Geng et al. (2019).① and ② are DEM sections of Loulan City and LK City surrounded by abandoned river channels shown in cyan. The shorelines are visible as similar concentric circles. One large salt pond is located in the northeast part of the lake basin in Magenta.
(For interpretation of the references to colour in this figure, the reader is referred to the web version of this article.).

reached a pH value of 7, and then 4–11 μm polymineral grains were separated using Stokes' law. To extract the fine-grained quartz, these polymineral grains were immersed in 30% hydrofluorosilicic acid (H2SiF6) for 3–5 days. Finally, the purified quartz was deposited on stainless steel discs with a diameter of 9.7 mm using ethanol before measurement. The regenerated infrared stimulated luminescence (IRSL) signal that is indistinguishable from the background, the obvious 110 °C (at 5 °C/s heating rate) thermoluminescence (TL) peak, and the OSL IR depletion ratio (Duller, 2003) ranged from 0.9 to 1.1 within uncertainties, together indicating that the chemically-isolated quartz is sufficiently pure for OSL dating (Fig. S1).

All OSL measurements were carried out using an automated Daybreak 2200 OSL reader equipped with infrared (880 ± 60 nm) and blue (470 ± 5 nm) LED units and a $^{90}Sr/^{90}Y$ beta source for irradiation. The quartz grains were stimulated for 60 s at 125 °C with blue LEDs (power ~45 mW/cm^2). The OSL decay curve detected the OSL signal using an EMI 9235QA photomultiplier tube coupled in front with two 3-mm U-340 (290–370 nm) glass filters. The OSL signal was calculated by subtracting the last 2-s integral from the first 2-s integral.

The De was determined using the single-aliquot regenerative-dose (SAR) protocol (Table S1; Murray and Wintle, 2000; Wintle and Murray, 2006). Preheat and cut-heat temperatures of 260 ºC and 220 ºC for 10 s were selected for the natural/regenerative dose, and the test dose, respectively (Table S1). This temperature choice has been widely adopted and accepted for fine-grain quartz (e.g., Lu et al., 2017; Kang et al., 2015, 2018). To remove any of OSL signal buildup during cycles of irradiation, preheat, and stimulation, and optical stimulation at 280 ºC for 10 s was applied at the end of each measurement cycle (Table S1). The effectiveness and reliability of SAR protocol in obtaining a De were checked by various routine checks, including dose recovery, recycling ratio, recuperation ratio, and overdispersion (Fig. S2).

A laboratory regenerative dose, close to the corresponding natural dose, was well retrieved for 11 representative samples (Fig. S2a). Within uncertainties, recycling ratios generally ranged from 0.9 to 1.1 (Fig. S2b), indicating that quartz OSL sensitivity changes during measurements were effectively rectified by the OSL signal from the test dose (Table S1). The low recuperation ratio, which was less than 5% for most of the samples, indicates that thermal transfer is negligible (Fig. S2c). Most of the samples had less than 10%, while 23 samples had none, showing the similarity of De between aliquots and possible good bleaching characteristics before sample burial. The fine-grain quartz OSL signal declined rapidly (Fig. S3a), indicating a fast component-dominated nature, beneficial for the SAR OSL dating protocol (Wintle and Murray, 2006). Dose-response curves for all samples were expressed using an exponential function, and ~10 aliquots were used for De determination, as presented for a typical sample LN034 (Fig. S3). Des from all the aliquots of each sample were normally distributed in general, as shown in Fig. S3c. The Des that resulted were generally lower than ~20 Gy (Table S2),

Table 1
Summary of collected samples and their corresponding age.

Site No.	Latitude	Longitude	Depth (m)	Sediment type	Material type	Dating method	Age (C.E.)
1	40°00'34.044''	90°58'22.66''	2.00	lacustrine	quartz	OSL	-4353 ± 557
2	41°00'53.34''	91°10'3.45''	3.20	lacustrine	quartz	OSL	-4179 ± 468
			4.70	lacustrine	quartz	OSL	-4462 ± 762
3	40°31'49.9''	90°57'11.88''	0.84	aeolian	quartz	OSL	-239 ± 200
			1.24	aeolian	quartz	OSL	-2806 ± 477
4	40°31'46.39''	90°57'13.83''	0.72	aeolian	quartz	OSL	470 ± 157
5	40°30'31.03''	90°54'27.86''	0.75	aeolian	quartz	OSL	529 ± 165
6	40°22'35.2''	90°51'27.54''	1.10	aeolian	quartz	OSL	660 ± 101
7	40°13'39.48''	90°39'26.54''	0.50	aeolian	quartz	OSL	1012 ± 67
			0.74	aeolian	quartz	OSL	995 ± 82
			1.00	lacustrine	quartz	OSL	986 ± 82
8	40°00'33.48''	90°58'22.5''	0.50	aeolian	quartz	OSL	1282 ± 61
9	40°20'13.7''	90°41'9.53''	1.00	aeolian	quartz	OSL	1490 ± 37
			1.30	lacustrine	quartz	OSL	932 ± 79
			1.77	lacustrine	quartz	OSL	-620 ± 195
10	40°12'55.26''	90°29'51.57''	0.26	lacustrine	quartz	OSL	1494 ± 38
			0.66	aeolian	quartz	OSL	367 ± 120
11	40°8'26.36''	90°30'3.91''	0.30	lacustrine	quartz	OSL	1494 ± 38
			0.55	aeolian	quartz	OSL	781 ± 85
12	40°12'56.42''	90°16'35.17''	0.45	lacustrine	quartz	OSL	1565 ± 32
			0.82	aeolian	quartz	OSL	458 ± 112
13	40°00'3.98''	90°17'26.67''	0.70	lacustrine	quartz	OSL	1687 ± 26
			0.85	lacustrine	quartz	OSL	1704 ± 24
14	40°14'8.32''	90°40'35.97''	0.50	aeolian	quartz	OSL	1693 ± 28
			0.95	lacustrine	quartz	OSL	641 ± 102
15	40°4'58.2''	90°25'0.48''	0.20	lacustrine	quartz	OSL	1706 ± 24
			0.30	lacustrine	quartz	OSL	1376 ± 46
			0.45	aeolian	quartz	OSL	1242 ± 57
16	40°07'9.91''	90°21'27.71''	0.28	aeolian	quartz	OSL	1838 ± 13
			0.36	aeolian	quartz	OSL	1587 ± 30
			0.46	lacustrine	quartz	OSL	1463 ± 38
			0.52	aeolian	quartz	OSL	1595 ± 29
			0.60	aeolian	quartz	OSL	1373 ± 44

All the samples were dated using OSL (Optically Stimulated Luminescence).

which was far lower than the De saturation level (Murray and Wintle, 2000; Wintle and Murray, 2006).

For dose rate calculation, the concentrations of U and Th were measured using Inductively Coupled Plasma Mass Spectrometry, and X-ray Fluorescence was used to determine the K concentration. The dose-rate conversion factor was based on Guérin et al. (2011). The fine-grained quartz was assumed to have an α-value of 0.04 (Rees-Jones, 1995). The cosmic dose rates were calculated using the equations presented by Prescott and Hutton (1994). A saturation water content was used for each sample, considering the depositional context, such as the lacustrine nature and the existence of a great lake in the past hundreds of years. The dose rate was calculated using the online Dose Rate and Age Calculator (DRAC; Durcan et al., 2015). Finally, by dividing the measured De by the dose rate, the quartz OSL age was determined. The OSL dating results are given in Supplemental Table S2.

2.2.3. Radiocarbon dating

Teeth, bones, horns, and pottery shards were found all over the LK city wall. Four kinds of animal relicts were collected at LK City, including the teeth of an *Equus ferus Caballus*, a *Camelus bactrianus* and a *Gazella subgutturosa*, and horns of *Ovis aries* (Table 2). Their species were identified, and the samples were sent to the BETA Analytical laboratory in Miami, Florida for Accelerator Mass Spectrometry (AMS) radiocarbon dating. All dating results fall within the range of available calibration data and are calibrated to calendar years (cal C.E.). Calibration was calculated using one of the databases associated with the 2013 INTCAL program. OSL dating of aeolian and lacustrine deposits and ^{14}C dating of animal relicts determined the age of the shorelines.

3. Results

3.1. Subsurface shoreline detection

The upper-most shoreline of Lop Nur was defined through the combined interpretation of SAR images and intensive ground truth checking (Gao et al., 2014; Gong et al., 2013, 2014; Liu et al., 2015; Liu et al., 2016a, 2016b; Shao et al., 2012), shown as a light blue line in Fig. 3, mainly determined by the presence of salt crusts. Using the upper-most shoreline as a boundary, we calculated that the total acreage of Lop Nur at its largest is 11,602 km^2. This figure is much larger than the 5350 km^2 reported by Xia (2007). Fig. 4 shows the DEM generated by the TanDEM-X mission. At an elevation of 792 m, this is the upper-most shoreline of the lake. Outside of this boundary, there are no salt crusts.

In addition, the SAR images revealed a detailed, vertical sequence of shorelines that records the historical changes in water levels in Lop Nur. Many of the ancient shorelines are buried beneath aeolian sediments but are apparent on the SAR images as bright curved features with a high salt content or light grey curved features composed of less salt and more silt.

The SAR image reveals three main belts (groups) of shorelines within the Lop Nur basin. The highest water levels formed this outermost belt of shorelines. This area exhibits the largest region of salty lacustrine deposits. The intermediate belt forms the ear-like feature defined by the green lines on Fig. 3, whereas the inner-most belt, associated with West Lake by dark blue lines, lies within the light blue line and partly truncates the green line.

The SAR images reveal a few buried shorelines hidden beneath dark lacustrine deposits along the western margin of the lake, referred to as West Lake. The dark deposits are free of salt crusts and have been interpreted as the youngest lacustrine deposits contained within West Lake. These younger deposits are superimposed on older and brighter lacustrine deposits within the area referred to as East Lake (Fig. 3). After the complete desiccation of East Lake, an interannual flood from upstream formed the relatively new West Lake on the west part of East Lake. West Lake's lacustrine deposits truncate the circular, continuous, closed shorelines of East Lake (Fig. 5), ultimately transforming East Lake into the shape of a human ear at a later stage.

3.2. OSL and radiocarbon dating results

Table 1 and Fig. 6 show the results of the OSL, and Table 2 shows the results of AMS ^{14}C dating. Lacustrine deposits were collected and dated at three sites within the basin of Lop Nur containing the shorelines in the ear-like feature: Site 14 (641 C.E.), Site 9 (932 C.E.), and Site 7 (986 C.E.). At site 11, only aeolian deposits were dated (781 C.E.); the dating of underlying lacustrine deposits failed. The four dated locations show that Lop Nur has never recovered to the highest water level marked by the upper-most shoreline since then.

The samples were dated using AMS ^{14}C radiocarbon methods, with calibrated ages.

The alluvial apron at Site 8 also marks a wet period that followed the lake's highest water levels. These deposits truncate and are superimposed on the receding shorelines found topographically below Site 6. Only the shorelines near the alluvial apron were eroded; those further north remained unchanged. Thick, sandy aeolian deposits that overlaid the alluvial apron were collected for dating and

Table 2
Samples of animal relicts and their corresponding age.

Site No.	Latitude	Longitude	Animal	Material type	Dating method	Age (C.E.)
17	40°05'41.7''	89°40'12.4''	*Gazella subgutturosa*	tooth	^{14}C	420–580
			Equus ferus Caballus	tooth	^{14}C	430–600
			Ovis aries Aries	horn	^{14}C	400–550
			Camelus bactrianus	tooth	^{14}C	550–650

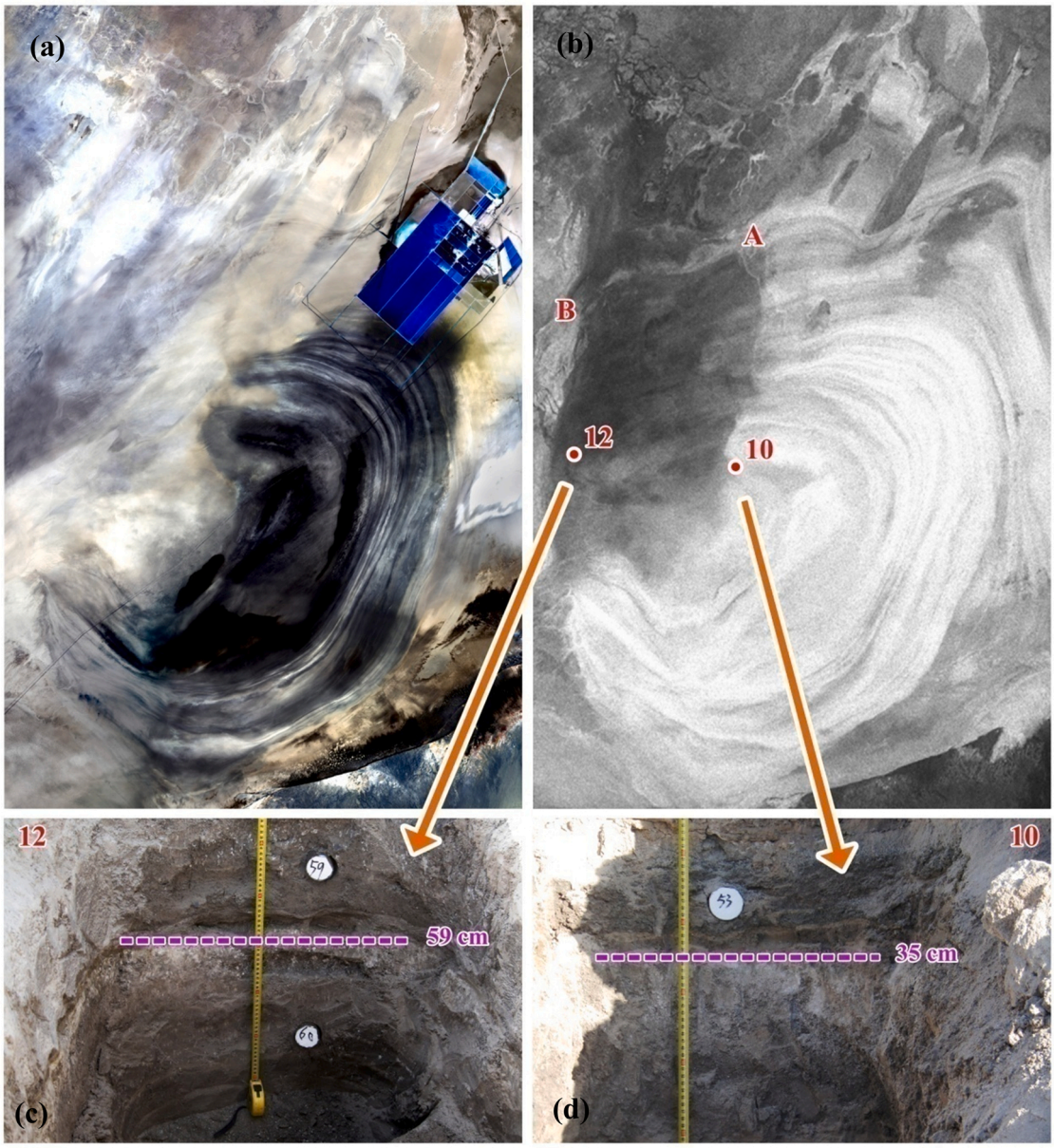

Fig. 5. The relationship between the sediments of the West Lake and the East Lake. (a) Optical remote sensing image of Lop Nur (GF-1©CNSA); (b) SAR image of Lop Nur RADARSAT-1 ©CSA.; (c) profile photo of site 12; (d) profile photo of site 10. Light grey shorelines continuously extend from site 10 to site 12, as do other shorelines (such as from Point A to Point B, although West Lake lacustrine deposits buried them). The purple dash line on the lower photographs is a layer of salt crust, in between lacustrine sediments and sandy lacustrine sediments of West Lake, which represents Lop Nur, was completely dried up, and salt crusts formed. (For interpretation of the references to colour in this figure, the reader is referred to the web version of this article.)

were dated to 1282 C.E.

SAR images show that the alluvial sediments were deposited by a river flowing northward from the Altun Mountains into Lop Nur. Given that these deposits underlie the dated Aeolian sediments, they must have been deposited before 1282 C.E. Dates obtained at Site 9 (932 C.E.), and Site 7 (986 C.E.) suggest that the deposition by this and other rivers in the area delivered water to Lop Nur until about 990 C.E.

The third hydrologic stage is represented by the West Lake deposits, which encompass an area of 1483 km^2 (Fig. 4). The lacustrine deposits collected at sites 11, 15, and 16 dates to 1494, 1376, and 1463 C.E., respectively. The top layer of lacustrine sediment at Site 13 dates between 1687 and 1704 C.E., whereas Site 15 dates to 1706 C.E.

Fig. 5 compares the optical remote sensing image with a SAR image of RADARSAT 1, taken in 1997. Shorelines extend from site 10

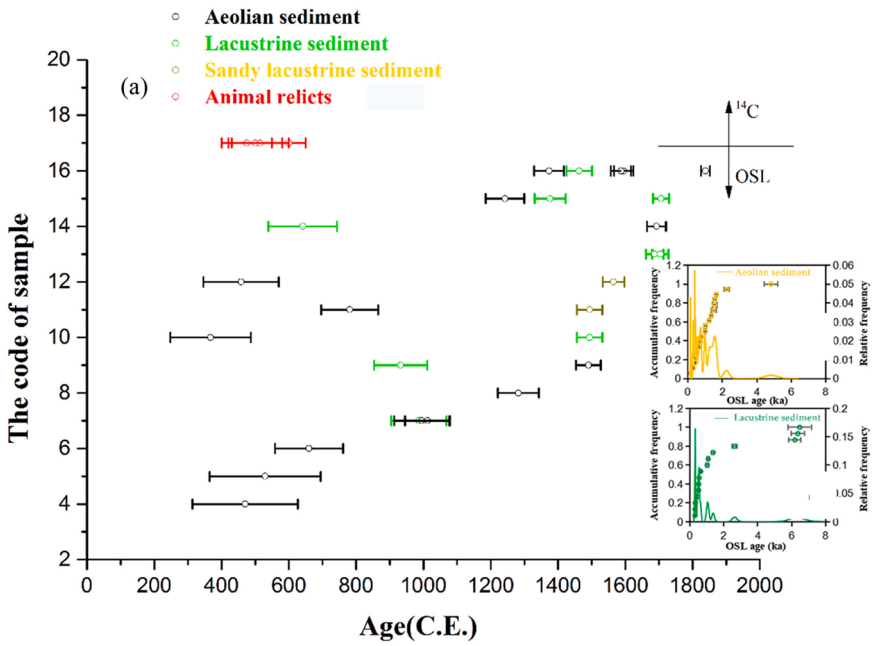

Fig. 6. (a) Dating results of OSL and ^{14}C at each sampling site. Dated aeolian sediments and dated animal or plant relicts found LK City indicate the lakebed was exposed and are suggestive of dry conditions. Dated lacustrine sediment is representative of lake conditions. Note, Sites 10 and 12, characterized by aeolian sediments, experienced dry conditions between 367 and 458 C.E., whereas lake conditions existed between 1494 and 1565 C.E. (b) Aeolian sediments OSL age frequency chart. (c) OSL age frequency chart for lacustrine sediments.

to site 12, as do other shorelines, such as from Point A to Point B, although West Lake lacustrine deposits buried them. The field photos show the interface between the sediments of the West Lake and the East Lake (Fig. 7).

4. Discussion

4.1. The past 2000 years of Lop Nur dynamics, including the lake-level changes and the driving forces

We have delineated shorelines and detected several buried shorelines in Lop Nur using the Canadian RADARSAT 1 and 2 satellite C-band Synthetic Aperture Radar and the Japanese Advanced Land Observing Satellite Phased Array type L-band Synthetic Aperture Radar (ALOS/PALSAR) images. Both C and L band radar can penetrate from half a meter to several meters of low electrical loss material such as dry aeolian sand (Blom et al., 1984; Elachi et al., 1984; Farr et al., 1986; McCauley et al., 1983; Skonieczny et al., 2015), and dry salt crusts (Shao et al., 2012). Thus, subsurface shorelines located above buried wet sediments or brine waters can be effectively identified and mapped. Dielectric constant and the roughness of the target are the main determinants of the brightness of SAR images. Wet material has a higher dielectric constant than dry material. The former delivers strong echoes back to the SAR instrument, generating high-bright features on the image, as well as allowing the lake basin to be distinguished from surrounding geomorphological features.

Microwaves reached the buried, moist saline layer of sediments in the lake basin because they exhibited a very high dielectric constant that acted as a strong reflector and generated strong signals back to the SAR antenna. Polarimetric information from shorelines shows that volume scattering made up nearly half of the total echo energy (Gao et al., 2014; Gong et al., 2013, 2014; Liu et al., 2015, 2016a, 2016b; Shao et al., 2012), which confirms that the signal partly comes from underneath sediments because of wave penetration.

The timing and magnitude of lake level changes during the late Holocene were determined by dating the age of selected shoreline deposits identified on the SAR images. The sequence of shorelines was obtained by field observation and analysis of samples of aeolian and lacustrine sediments, salt crusts, salt crystals, and brine collected over ten field trips around twelve years.

Following its high stand, Lop Nur exhibited three major water level stages, corresponding to periods of relatively dry, wet, and dry (Fig. 6). The first stage is referred to herein as “the Lop Nur Stage.” The lacustrine samples within the lake basin were collected at sites 1 and 2, and the aeolian samples of Yardan collected at site 3 date to 4000 B.C.E., as shown in magenta points in Fig. 3. They represent the wet period before the lake’s desiccation. Site 4 is located within the highest (most peripheral) shoreline boundary. The upper sediment layers within the shoreline dates to 470 C.E. At sites 10 and 12, a layer of salt crust is positioned between the sandy lacustrine sediment layer and the second lacustrine layer, the latter of which dates to between 367 and 458 C.E. (similar to Site 4, see Table 1), as shown in Fig. 6. In that period, the exposed lakebed sediments were buried by windblown materials. Data obtained from the aeolian sediments suggest that Lop Nur was completely dry between 367 and 470 C.E. After this dry period, Lop Nur refilled before water levels

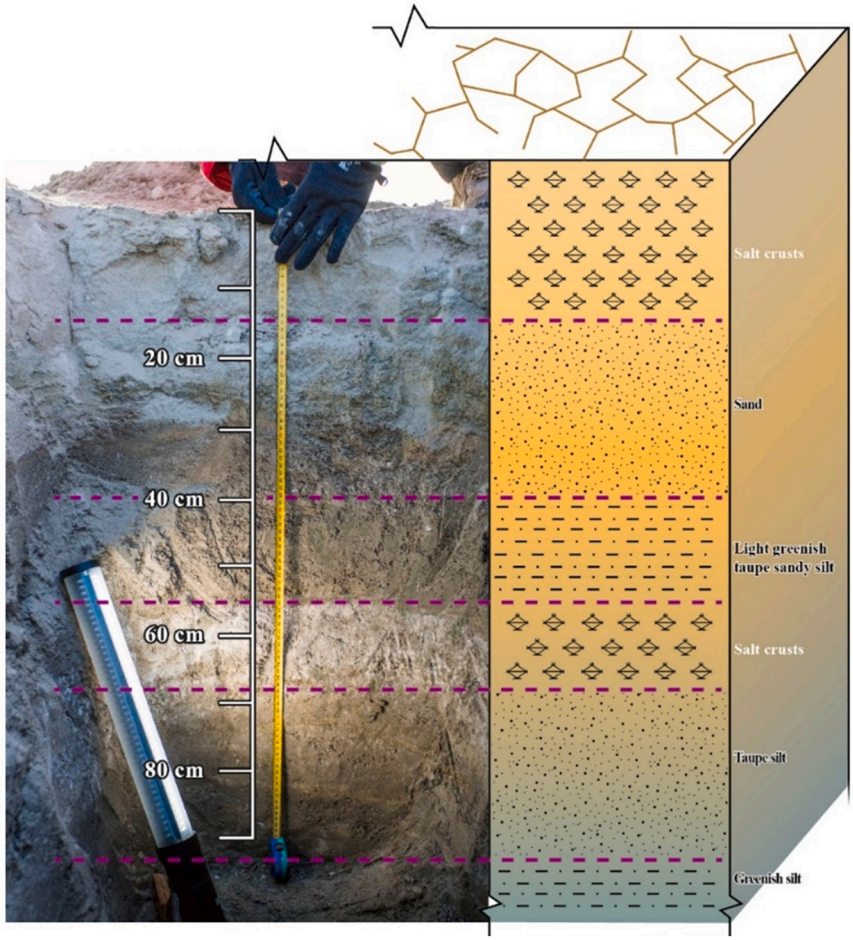

Fig. 7. Stratigraphic section at Site 12 shows typically observed sedimentary deposit variations. Aeolian sediment at a depth of 0.85 m dates to 458 C.E., while sandy lacustrine sediment at a depth of 0.45 m dates to 1565 C.E.

declined again, at which time two shorelines formed. One shoreline was defined in the field at Site 5, the second at Site 6 (Fig. 3 and Table 1). The subsurface layers of aeolian sediments at Sites 5 and 6 dates to 529 and 660 C.E., respectively.

According to the distribution of the shorelines and their spatiotemporal relationship with the dated samples, we hypothesized that before approximately 360 C.E., there was sufficient water entering Lop Nur from eastward-flowing rivers to fill it to its maximum level (Fig. 3). Elevated water levels during this time are supported by "The Memoir on the Western Regions" within the Book of Han, written during the Eastern Han Dynasty (202 B.C.E.–220 C.E.) (Yu, 2014). It states that:

"Eastward it flows into the Puchang Sea." Another name for the Puchang Sea is Salt Marsh. It is more than 300 li (1 li = 415.8 m, 300 li = 124.74 km) from the Yumen and Yang Barriers and measures 300 li in width and length. Its waters remain stagnant and are not increased or reduced in winter or summer".

The diameter of Lop Nur, measured on SAR images and based on the outer-most shorelines, is about 170 km. The measurement record in the Book of Han cannot be verified, the recorded number is in an order of magnitude with our result.

Following this high stage, the Lop Nur region entered a dry period between 360 and 470 C.E. (Fig. 6). Historical records indicate that the region became a harsh, desolate place because dramatically decreasing precipitation led to severe water shortages in upstream regions (Yang et al., 2006a; Zhang et al., 2012). Lop Nur is said to have vanished, and Loulan, LK, LE, and Tuyin City and other smaller cities within the Loulan Kingdom were vacated (Hedin, 1905, 1903; Lü et al., 2010; Mischke et al., 2017; Samuel, 1994; Stein, 1907, 1921,1928; Xia et al., 2007). The Loulan Kingdom is also referred to as Shan-shan in "A Record of the Buddhistic Kingdom" written by Monk Fa-Hien (Giles, H. A, 1923). Monk Fa Hien set out from Chang'an (Today's Xi'an) in 399 C.E. and arrived in Shan-shan several months later. He wrote,

> "There are many evil demons and hot winds,. There is not a bird to be seen in the air above, nor an animal on the ground below. Though you look all round most earnestly to find where you can cross, you know not where to make your choice, the only mark and indication being dry bones of the dead (left upon sand)."

Notably, Monk Fa Hien mentioned "hot wind" in his book. Historical records show that this region has not been suitable for

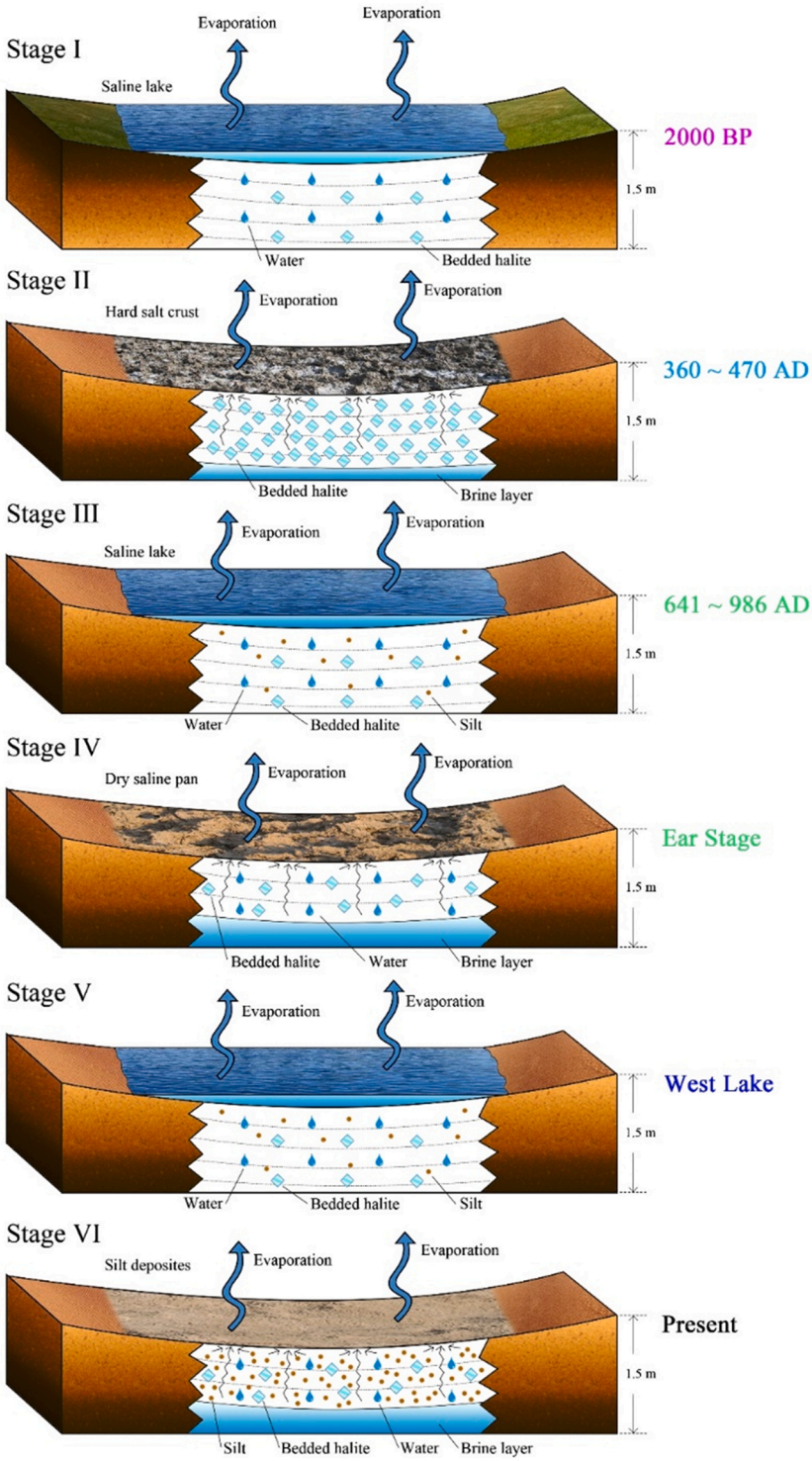

Fig. 8. The Evolution of Lop Nur and salt crusts. Stage I: wet period, prior to the lake's desiccation. Stage II: dry period, lake completely dried and surface sediments characterized by thickest (thickness >1 m) and hardest salt crusts with well-eroded surfaces, photo taken at point α; similar salt crusts were found at point β and site 2 shown in Fig. 3. Stage III: wet period, lake replenishment. Stage IV: dry period, forming the ear features and moderately hard salt crusts with thicknesses less than 1 m, such as at point γ. Stage V: lake refilled. Stage VI: lacustrine sediments consisting of loose silt and sand, such as at point δ of West Lake.

habitation since the beginning of this dry period. However, our paleo-lake data shows that the lake went through a phase of renewed filling after a dry period. The rise in lake levels shaped the portion of Lop Nur that created the morphologic features that appear in the shape of a human ear on the SAR images as well as those shorelines where lacustrine deposits were collected at Sites 14 (641 C.E.), 9 (932 C.E.), and 7 (986 C.E.). The dated materials suggest that the area was inundated by around 640 C.E. before lake levels subsequently declined to form the topographically lower shorelines between sampling Sites 8 and 6.

During this time, alluvial sediments truncated and were superimposed on the shorelines at Site 8 (see Fig. 3). Although only the shorelines near the alluvial apron were truncated, the alluvial apron had eroded the shoreline correlative with that at Site 6, indicating that rivers flowed into the lake up to the time when the shoreline at Site 6 was formed. The only datable material at Site 8 was collected from thick sandy aeolian deposits that buried the alluvial apron. The aeolian sediments dates to 1282 C.E. However, the SAR images show that the river channel that formed this alluvial apron flowed northwards from the Altun Mountains into Lop Nur long before 1282 C.E. For example, dated samples collected at Site 9 (932 C.E.) and Site 7 (986 C.E.) suggest that these and other rivers brought water to the lake in the middle of the 10th century. Afterward, Lop Nur shrank, forming the "ear-shaped" shorelines. The absence of more recent alluvial deposits indicates that the recession of Lop Nur began after 990 C.E. This drying process represents the second stage—the "ear stage"— which covers a maximum area of 2171 km^2 and is buried beneath the lacustrine deposits of the West Lake (Fig. 3).

The third major lake level is represented by the shorelines of West Lake and covers an area of 1483 km^2 (Fig. 6). Since the early 1700 s, the lake has been a river-controlled small lake. During this time, seasonal and annual flooding, wet airflow, and rainfall arrived in Lop Nur from time to time (Li et al., 2018; Xia, 2007). After this wet period, the West Lake of Lop Nur began to shrink. An abandoned river channel is apparent on the DEM (Fig. 4), entering Lop Nur from the south to the north and is located nearby Site 16. The depth of this riverbed is only 50 cm measured from DEM, but its width reaches 1 km. As shown by aerial photos taken in the 1950s and USA Corona photos taken in the 1960 s, West Lake occasionally received flood water and wet airflow, causing water to be randomly distributed within the West Lake area. Lop Nur became completely dry before 1972 (Xia, 2007). The wet-dry-wet-dry cycle of Lop Nur is depicted in Fig. 8 demonstrated based on the evolution of observed and modeled salt crusts. The analysis assumes that the different shapes and hardness of the salt crusts express their age. The harder the salt crusts, the older they are. Their evolution processes are illustrated in Fig. 8.

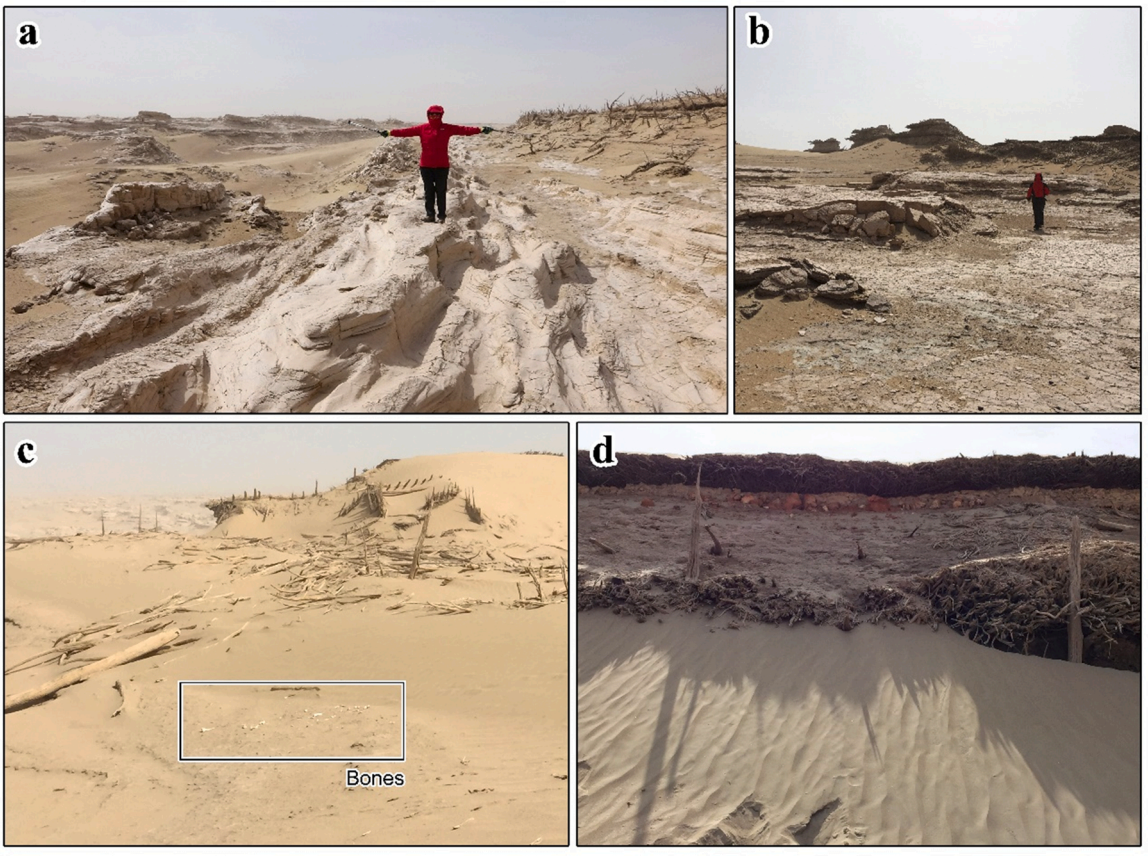

Fig. 9. Field photos obtained along the way to LK City. (a) River terraces with dead Rose Willow near LK City; (b) LK city's in the distance; (c) scattered bones, teeth, and horns in the center of LK City; and (d) closer look at the city wall with red bricks.(For interpretation of the references to colour in this figure, the reader is referred to the web version of this article.)

4.2. The linkage between the Lop Nur's reduction and the decline of the ancient Loulan Kingdom

Historical records and archaeological excavations of ruins in the region indicate that the Loulan Kingdom disappeared in 500 C.E. Our dating results of the shorelines shown on multiple space-borne SAR images indicate that Lop Nur had vanished by 470 C.E., presumably in response to a decline in runoff from upstream rivers in its catchment. Thus, the progressive disappearance of the Lop Nur was temporally correlative with the demise of the Loulan Kingdom. In September 2015, we first visited the LK City (Site 17). We found a large number of animal relicts strewn across the ground surface. Animal bones, teeth, and horns collected within LK City were dated to 475, 500, 515, and 600 C.E. (see Table 2), using an AMS^{14}C radiocarbon technique. The OSL records of the aeolian sediment from Sites 4, 5, 10, and 12 show a remarkable spatiotemporal relationship with the AMS records of the animal relicts at Site 17 (Fig. 9). These animal relicts provide additional evidence of the timing of the demise of the Loulan Kingdom in that they are correlative with the first stage of Lop Nur, as shown in red points in Fig. 3 and Fig. 6.

The Lop Nur catchment was an important section of the ancient "Silk Road". Especially during the Great Han Dynasty (Hill, 2009), it was the only route for trade caravans. The desertion of Lop Nur, the abandonment of the Central Route of the "Silk Road," and the sudden collapse of the Loulan Kingdom have been the subject of intense debate in both social and natural science (Dong et al., 2012; Xia, 2007; Mischke et al., 2017). Our data show that Lop Nur, which initially covered an area of more than 11,602 km^2, started to shrink at 360 C.E. and eventually vanished around 500 C.E. Chronologic studies in adjacent regions supported our conclusion that the main cause of the disappearance of Lop Nur is climate change, and human activities (Mischke et al., 2017) may aggravate climate deterioration.

The drought event in Lop Nur is consistent with the warm and dry period of 0–500 C.E. in the history of Xinjiang. The sediment dating analysis of Bosten Lake shows that after 200 C.E., the climate began to turn into a warm and dry period, and the hydrodynamic intensity of Bosten Lake declined sharply at about 400–700 C.E. (Xie et al., 2021). During this period, the culture of the Loulan Kingdom collapsed. The Lop Nur drying event has also been recorded in tree-ring chronologies and lake sediments of the Tibetan Plateau (Chen et al., 2008; Liu et al., 2016a, 2016b; Sheppard et al., 2004; Yang et al., 2006a, 2006b, 2014; Yin et al., 2016; Zhang et al., 2013). Dendroclimatic annual precipitation records indicate that widespread, predominately drier conditions existed throughout the 4th to 6th centuries within the north-eastern Tibetan Plateau (Yang et al., 2014). Annual precipitation reconstructed from juniper trees, for example, indicates relatively dry years occurred in 426–500 C.E. in north-eastern Qinghai Province (Sheppard et al., 2004). Centennial scale dry periods, including 425–520 C.E. have also been identified in the north-eastern Tibetan Plateau's Qaidam Basin (Yin et al., 2016). In addition, paleoclimatic records show that most lakes within the current mid-latitude arid Asian region experienced extensive moisture between 6000 B.C.E – 2000 B.C.E. This humid period was followed by a consistent decrease in moisture to the present (Chen et al., 2008). The late Holocene lacustrine sediments of the southern Tarim Basin also suggest that the extent of wetlands today is considerably smaller than before. It is assumed that changes in moisture are associated with global westerlies (Yang et al., 2006a, 2006b). The lake was refilled with water several times during this interval, but the region has since become nearly uninhabitable. Several studies show that climate change in Xinjiang alternately occurs in cold and wet periods and in warm and dry periods. In the cold and wet periods, the precipitation and the water volume of rivers and lakes increased. In the warm and dry periods, the water volume of rivers and lakes decreased and western civilization declined.

The regional reduction in moisture also coincides with a time when central China experienced the most severe period of chaotic warfare in the course of Chinese civilization (Dien, 1991; Ge, 2011; Lü, 2005), that is, the Southern-Northern Dynasty (420–589 C.E.). This period is known for its extreme warfare between the Han nationality and other nationalities, frequent transitions of kingship among several kingdoms, the rise and fall of many smaller kingdoms, and a dramatic decline in population because of both warfare and the serve drought that occurred across the central plains (Ge, 2011; Yu, 2014) of China.

5. Conclusion

This paper focuses on examining the past and present problems of Lop Nur's hydrological dynamics and their impacts on oasis civilization. The OSL dates of both aeolian and lacustrine sediments reveal that the lake level of Lop Nur has been unstable over the last two millennia. The Lop Nur once covered an area of more than 11, 602 km^2 as suggested by spaceborne SAR data. The largest lake-level seems to be shrunken gradually during 360–470 C.E. After that, there were several fluctuations of lake level but never reached the upper-most shorelines. Based on the chronological coupling between lake-level change and ancient human settlement, we extrapolate that the dramatic hydrological changes of the Lop Nur catchment may have a profound influence on the historic oasis states (e.g., the Loulan kingdom) along the ancient Silk Road.

CRediT authorship contribution statement

Yun Shao: Writing – original draft. **Huaze Gong:** Investigation. C**harles Elachi:** Formal analysis. **Brian Brisco:** Data curation. **Jiaqi Liu:** Investigation. **Xuncheng Xia:** Investigation. **Huadong Guo:** Writing – original draft. **Yuyang Geng:** Data curation. **Shugang Kang:** OSL dating. **Chang-an Liu:** Data curation. **Zhi Yang:** Data Curation. **Tingting Zhang:** Writing – review & editing.

Declaration of Competing Interest

The authors declare that they have no known competing financial interests or personal relationships that could have appeared to influence the work reported in this paper.

Acknowledgments

We thank Z. Gao, L. Wang, A. Cai, T. Zhang, L. Liu, G. Wang, Z. Wan, K.X, H. Lü, X. Qin, Z. Gu, G. Mu, A. Kurban, Y. Zhao, Z. Jiang and N. Li; BETA laboratory for conducting the ^{14}C analyses. Y. Shao, H. Z. Gong and H. D. Guo interpreted the SAR images and wrote the manuscript, C. Elachi and B. Brisco analyzed the polarimetric data, X. Xia and J. Liu led the field campaigns, S. Kang made the OSL dating, Y. Y. Geng, C. A. Liu, Z. Yang, and T. T. Zhang processed SAR images and samples. This research was supported by the Ministry of Science & Technology [2016YFB0502500, 2007AA12Z168, and 2014FY210500], National Science Foundation of China [42071313, 41431174, U1303285] and the Youth Innovation Promotion Association CAS (2018447).

Appendix A. Supporting information

Supplementary data associated with this article can be found in the online version at doi:10.1016/j.ejrh.2022.101002.

References

Blom, R.G., Crippen, R.E., Elachi, C., 1984. Detection of subsurface features in SEASAT radar images of Means Valley, Mojave Desert, California. Geology 12 (6), 346–349.
Buckley, B.M., Anchukaitis, K.J., Penny, D., Fletcher, R., Cook, E.R., Sano, M., Le, C.N., Wichienkeeo, A., Ton, T.M., Truong, M.H., 2010. Climate as a contributing factor in the demise of Angkor, Cambodia. Proc. Natl. Acad. Sci. USA 107 (15), 6748–6752.
Büntgen, U., Tegel, W., Nicolussi, K., McCormick, M., Frank, D., Trouet, V., Kaplan, J.O., Herzig, F., Heussner, K.U., Wanner, H., Luterbacher, J., Esper, J., 2011. 2500 years of European climate variability and human susceptibility. Science 331 (6017), 578.
Chen, F.H., Yu, Z.C., Yang, M.L., Ito, E., Wang, S.M., Madsen, D.B., Huang, X.Z., Zhao, Y., Sato, T., Birks, H.J.B., 2008. Holocene moisture evolution in arid central Asia and its out-of-phase relationship with Asian monsoon history. Quat. Sci. Rev. 27 (3–4), 351–364.
Chen, X.L., 2014. Loulan Archaeology. University Press, Lanzhou.
Chu, G.Q., Liu, J.Q., Sun, Q., Lu, H.Y., Gu, Z.Y., Wang, W.Y., Liu, T.S., 2002. The 'Mediaeval Warm Period' drought recorded in Lake Huguangyan, tropical South China. Holocene 12 (5), 511–516.
Cook, E.R., Woodhouse, C.A., Eakin, C.M., Meko, D.M., Stahle, D.W., 2004. Long-term aridity changes in the Western United States. Science 306 (5698), 1015–1018.
Demenocal, P.B., 2001. Cultural responses to climate change during the late Holocene. Science 292 (5517), 667–673.
Dien, A.E., 1991. State and Society in Early Medieval China. Stanford University Press.
Dong, Z.B., Ping, L., Qian, G.Q., Xia, X.C., Zhao, Y.J., Mu, G.J., 2012. Research progress in China's Lop Nur. Earth-Sci. Rev. 111 (1–2), 142–153.
Duller, G.A.T., 2003. Distinguishing quartz and feldspar in single grain luminescence measurements. Radiat. Meas. 37 (2), 161–165.
Durcan, J.A., King, G.E., Duller, G.A.T., 2015. DRAC: dose rate and age calculator for trapped charge dating. Quat. Geochronol. 28, 54–61.
Elachi, C., Roth, L.E., Schaber, G.G., 1984. Spaceborne radar subsurface imaging in hyperarid regions. IEEE Trans. Geosci. Remote Sens. 22 (4), 383–388.
Farr, T.G., Elachi, C., Hartl, P., Chowdhury, K., 1986. Microwave penetration and attenuation in desert soil: a field experiment with the shuttle imaging radar. IEEE Trans. Geosci. Remote Sens. 24 (4), 590–594.
Frankopan, P., 2015. The Silk Roads. Bloomsbury Publishing.
Gao, Z.H., Gong, H.Z., Zhou, X., Shao, Y., Yuan, M.H., Wang, L.F., 2014. Study on the polarimetric characteristics of the Lop Nur arid area using PolSAR data. J. Appl. Remote Sens 8 (1), 2610–2615.
Ge, Q.S., 2011. Climate Changes in Chinese history. Science Press, Beijing.
Geng, Y.Y., Shao, Y., Zhang, T.T., Gong, H.Z., Yang, L., 2019. High-resolution elevation model of Lop Nur playa derived from TanDEM-X. J. Sens. 9, 1–12.
Giles, H. A, 1923. The travels of Fa-hsien (399-414AD), or, Record of the Buddhistic Kingdoms. Cambridge University Press.
Gong, H.Z., Shao, Y., Brisco, B., Hu, Q.R., Tian, W., 2013. Modeling the dielectric behavior of saline soil at microwave frequencies. Can. J. Remote Sens. 39 (1), 17–26.
Gong, H.Z., Shao, Y., Zhang, T.T., Liu, L., Gao, Z.H., 2014. Scattering mechanisms for the "ear" feature of Lop Nur Lake basin. Remote Sens 6 (5), 4546–4562.
Guérin, G., Mercier, N., Adamiec, G., 2011. Dose-rate conversion factors: update. Anc. Tl 29 (1), 5–8.
Hedin, S.A., 1903. Central Asia and Tibet: towards the Holy City of Lassa. Hurst Black.
Hedin, S.A., 1905. Lop Nur: scientific results of a journey in central Asia (1889-1902). Vol. 2. K. Boktryckeriet, PA Norstedt Söner, Stockh.
Hill, J.E., 2009. Through the Jade Gate to Rome: A Study of the Silk Routes during the Later Han Dynasty 1st to 2nd Centuries. Book Surge Publishing.
Hodell, D.A., Brenner, M., Curtis, J.H., 1995. Possible role of climate in the collapse of classic Maya civilization. Nature 375 (6530), 391–394.
Kang, S.G., Wang, X.L., Lu, Y.C., Liu, W.G., Song, Y.G., Wang, N., 2015. A high-resolution quartz OSL chronology of the Talede loess over the past ~30 ka and its implications for dust accumulation in the Ili Basin, Central Asia. Quat. Geochronol. 30, 181–188.
Kang, S.G., Wang, X.L., Roberts, H.M., Duller, G.A.T., Cheng, P., Lu, Y.C., An, Z.S., 2018. Late Holocene anti-phase change in the East Asian summer and winter monsoons. Quat. Sci. Rev. 188, 28–36.
Lasne, Y., Paillou, P., Freeman, A., Farr, T., McDonald, K., Ruffie, G., Malezieux, J.M., Chapman, B., 2009. Study of hypersaline deposits and analysis of their signature in airborne and spaceborne SAR data: example of death valley, California. IEEE Trans. Geosci. Remote Sens. 47 (8), 2581–2598.
Li, B.Y., Gong, H.Z., Shao, Y., Li, L., Wang, L.F., Liu, C.A., Xie, K.X., 2015. The consistency between NA content distribution at the subsurface and the lake body's movement in Lop Nur. Int J. Digit Earth 9 (7), 662–675.
Li, K.K., Qin, X.G., Xu, B., Zhou, L.P., Jia, H.J., Mu, G.J., Wu, Y., Wei, D., Tian, X.H., Shao, H.Q., Li, W., Song, H.Z., Liu, J.Q., Jiao, Y.X., 2021a. Palaeofloods at ancient Loulan, northwest China: Geoarchaeological perspectives on burial practices. Quat. Int. 577, 131–138.
Li, K.K., Qin, X.G., Zhang, L., Gu, Z.Y., Xu, B., Jia, H.J., Mu, G.J., Lin, Y.C., Wei, D., Wang, C.X., Wu, Y., Tian, X.H., Lu, H.Y., Wu, N.Q., Jiao, Y.X., 2018. Hydrological change and human activity during Yuan–Ming Dynasties in the Loulan area, northwestern China. Holocene 28 (8), 1266–1275.
Li, K.K., Qin, X.G., Zhang, L., Wang, S.Z., Xu, B., Mu, G.J., Wu, Y., Tian, X.H., Wei, D., Gu, Z.Y., Wang, C.X., Zhang, J.P., Xu, D.K., Tang, Z.H., Lin, Y.C., Li, W., Liu, J.Q., Jiao, Y.X., 2019. Oasis landscape of the ancient Loulan on the west bank of Lake Lop Nur, Northwest China, inferred from vegetation utilization for architecture. Holocene 29 (6), 1030–1044.
Li, K.K., Qin, X.G., Xu, B., Wu, Y., Mu, G.J., Wei, D., Tian, X.H., Shao, H.Q., Wang, C.X., Jia, H.J., Li, W., Song, H.Z., Liu, J.Q., Jiao, Y.X., 2021b. New radiocarbon dating and archaeological evidence reveal the westward migration of prehistoric humans in the drylands of the Asian interior. Holocene 31 (10), 1555–1570.
Li, W., Mu, G.J., Lin, Y.C., Zhang, D.L., 2021. Abrupt climatic shift at ~4000 cal. yr B.P. and late Holocene climatic instability in arid Central Asia: evidence from Lop Nur saline lake in Xinjiang, China. Sci. Total Environ. 784, 147202.
Li, W., Mu, G.J., Zhang, W.G., Lin, Y.C., Zhang, D.L., Song, H.Z., 2019. Formation of greigite (Fe_3S_4) in the sediments of saline lake Lop Nur, northwest china, and its implications for paleo-environmental change during the last 8400 years. J. Asian earth Sci. 174, 99–108.
Liu, C.A., Gong, H.Z., Shao, Y., Li, B.Y., 2015. Detecting the depth of a subsurface brine layer in Lop Nur lake basin using polarimetric L-band SAR. J. Sens. https://doi.org/10.1155/2015/245790.

Liu, C.A., Gong, H.Z., Shao, Y., Yang, Z., Liu, L., Geng, Y.Y., 2016. Recognition of salt crust types by means of POLSAR to reflect the fluctuation processes of an ancient lake in Lop Nur. Remote Sens Environ. 175, 148–157.
Liu, C.L., Zhang, J.F., Jiao, P.C., Mischke, S., 2016. The Holocene history of Lop Nur and its palaeoclimate implications. Quat. Sci. Rev. 148, 163–175.
Lü, H.Y., Xia, X.C., Liu, J.Q., Qin, X.G., Wang, F.B., Yidilisi, A., Zhou, L.P., Mu, G.J., Jiao, Y.X., Li, J.Z., 2010. A preliminary study of chronology for a newly-discovered ancient city and five archaeological sites in Lop Nor, China. Chin. Sci. Bull. 55 (1), 63–71.
Lü, S.M., 2005. History of the Southern and Northern Dynasties in the 5th century. Guji Press,, Shanghai.
Lu, Y.C., Wang, X.L., Wintle, A.G., 2017. A new OSL chronology for dust accumulation in the last 130,000 yr for the Chinese Loess Plateau. Quat. Res. 67 (1), 152–160.
McCauley, J.F., Schaber, G.G., Breed, C.S., Grolier, M.J., Haynes, C.V., Issawi, B., Elachi, C., Blom, R., 1983. Subsurface valleys and geoarcheology of the eastern Sahara revealed by shuttle radar. Science 218, 1004–1020.
Mischke, S., Liu, C.L., Zhang, J.F., Zhang, C.J., Zhang, H., Jiao, P.C., Plessen, B., 2017. The world's earliest Aral-Sea type disaster: the decline of the Loulan Kingdom in the Tarim Basin. Sci. Rep. 7, 43102.
Mischke, S., Zhang, C.J., Liu, C.L., Zhang, J.F., Jiao, P.C., Plessen, B., 2019. The Holocene salinity history of Lake Lop Nur (Tarim Basin, NW China) inferred from ostracods, foraminifera, ooids and stable isotope data. Glob. Planet. Change 175, 1–12.
Murray, A.S., Wintle, A.G., 2000. Luminescence dating of quartz using an improved single-aliquot regenerative-dose protocol. Radiat. Meas. 32 (1), 57–73.
Prescott, J.R., Hutton, J.T., 1994. Cosmic ray contributions to dose rates for luminescence and ESR dating: large depths and long-term time variations. Radiat. Meas. 23 (2–3), 497–500.
Qin, X.G., Liu, J.Q., Jia, H.J., Lu, H.Y., Xia, X.C., Zhou, L.P., Mu, G.J., Xu, Q.H., Jiao, Y.X., 2011. New evidence of agricultural activity and environmental change associated with the ancient Loulan kingdom, China, around 1500 years ago. Holocene 22 (1), 53–61.
Rees-Jones, J., 1995. Optical dating of young sediments using fine-grain quartz. Anc. TL 13 (2), 9–14.
Samuel, B., 1994. SI-YU-KI: Buddhist Records of the Western World. Motilal Banarsidass Publisher.
Shao, Y., Gong, H.Z., Gao, Z.H., Liu, L., Li, L., Zhang, T.T., 2012. SAR data for subsurface saline lacustrine deposits detection and primary interpretation on the evolution of the vanished Lop Nur Lake. Can. J. Remote Sens. 38 (3), 267–280.
Shao, Y., Hu, Q.R., Guo, H.D., Lu, Y., Dong, Q., Han, C.M., 2003. Effect of dielectric properties of moist salinized soils on backscattering coefficients extracted from RADARSAT image. IEEE Trans. Geosci. Remote Sens. 41 (8), 1879–1888.
Sheppard, P.R., Tarasov, P.E., Graumlich, L.J., Heussner, K.U., Wagner, M., Osterle, H., Thompson, L.G., 2004. Annual precipitation since 515 BC reconstructed from living and fossil juniper growth of northeastern Qinghai Province, China. Clim. Dyn. 23 (7), 869–881.
Skonieczny, C., Paillou, P., Bory, A., Bayon, G., Biscara, L., Crosta, X., Eynaud, F., Malaize, B., Revel, M., Aleman, N., 2015. African humid periods triggered the reactivation of a large river system in Western Sahara. Nat. Commun. 6 (1) https://doi.org/10.1038/ncomms9751.
Stein, M.A., 1907. Ancient Khotan: Detailed Report of Archaeological Explorations in Chinese Turkestan. Clarendon Press, Oxford.
Stein, M.A., 1921. Serindia: Detailed Report of Explorations in Central Asia and Westernmost China. Clarendon Press, Oxford.
Stein, M.A., 1928. Innermost Asia: Report of Exploration in Central Asia Kansu and Eastern Iran. Clarendon Press, Oxford.
Touzi, R., Boerner, W.M., Lee, J.S., Lueneburg, E., 2004. A review of polarimetry in the context of synthetic aperture radar concepts and information extraction. Can. J. Remote Sens. 30 (3), 380–407.
Turner II, B.L., 1974. Lop Nur, China. Science 185 (4146), 118–124.
Wang, L.F., Gong, H.Z., Shao, Y., Li, B.G., 2014. Analysis of elevation discrepancies along the Lop Nur ear-shaped stripes observed using GLAS and DGPS data. Int. J. Remote Sens. 35 (4), 1466–1480.
Wintle, A.G., Murray, A.S., 2006. A review of quartz optically stimulated luminescence characteristics and their relevance in single-aliquot regeneration dating protocols. Radiat. Meas. 41 (4), 369–391.
Xia, X.C., Wang, F.B., Zhao, Y.J., 2007. Lop Nur. Science Press, China. Beijing.
Xie, H.C., Liang, J., Vachula, R.S., Russell, J.M., Chen, S.Q., Guo, M.J., Wang, X., Huang, X.Z., Chen, F.H., 2021. Changes in the hydrodynamic intensity of Bosten Lake and its impact on early human settlement in the northeastern Tarim Basin, Arid Central Asia. Palaeogeogr., Palaeoclimatol., Palaeoecol. 576, 110499.
Xu, B., Gu, Z.Y., Qin, X.G., Wu, Y., Mu, G.J., Jiao, Y.X., Zhang, L., Hao, Q.Z., Wang, L., Wei, D., Liu, J.Q., 2017. Radiocarbon Dating the Ancient City of Loulan. Radiocarbon 59 (4), 1–12.
Yancheva, G., Nowaczyk, N.R., Mingram, J., Dulski, P., Schettler, G., Negendank, J.F.W., Liu, J.Q., Sigman, D.M., Peterson, L.C., Haug, G.H., 2007. Influence of the Intertropical Convergence Zone on the East Asian monsoon. Nature 445 (7123), 74–77.
Yang, B., Qin, C., Wang, J.L., He, M.H., Melvin, T.M., Osborn, T.J., Briffa, K.R., 2014. A 3,500-year tree-ring record of annual precipitation on the northeastern Tibetan Plateau. Proc. Natl. Acad. Sci. USA 111 (8), 2903–2908.
Yang, X.P., Preusser, F., Radtke, U., et al., 2006. Late quaternary environmental changes in the Taklamakan desert, western China, inferred from OSL-dated lacustrine and aeolian deposits. Quat. Sci. Rev. 25 (9–10), 923–932.
Yang, X., Liu, Z., Mang, F., White, P.D., Wang, X., 2006. Hydrological changes and land degradation in the southern and eastern Tarim Basin, Xinjiang, China. Land Degrad. Dev. 17, 381–392.
Yin, Z.Y., Zhu, H.F., Huang, L., Shao, X.M., 2016. Reconstruction of biological drought conditions during the past 2847 years in an alpine environment of the northeastern Tibetan Plateau, China, and possible linkages to solar forcing. Glob. Planet Change 143, 214–227.
Yu, T., 2014. A concise commentary on memoirs on the western regions in the official histories of the Western and Eastern Han. Wei, Jin, and Southern and Northern Dynasties. The Commercial Press, Beijing.
Zhang, J.F., Liu, C.L., Wu, X.H., Liu, K.X., Zhou, L.P., 2012. Optically stimulated luminescence and radiocarbon dating of sediments from Lop Nur, China. Quat. Geochronol. 10 (4), 150–155.
Zhang, J.P., Lu, H.Y., Wu, N.Q., Qin, X.G., Wang, L., 2013. Palaeo environment and agriculture of ancient Loulan and Milan on the Silk Road. Holocene 23 (2), 208–217.
Zhang, T.T., Shao, Y., Gong, H.Z., Li, L., Wang, L.F., 2014. Salt content distribution and paleoclimatic significance of the Lop Nur "Ear" feature: results from analysis of EO-1 hyperion imagery. Remote Sens. 8 (6), 7783–7799.
Zhang, T.T., Shao, Y., Geng, Y.Y., Gong, H.Z., Yang, L., 2021. A study on historical location and evolution of Lop Nor in China with maps and DEM. J. Arid Land 13 (6), 639–652.